UDC 539.2: 669

[1*]Komarov F., [1]Vlasukova L., [1]Makhavikou M.,
[2]Wendler E., [3]Togambayeva A.

[1]Institute of Applied Physics Problems BSU, 7 Kurchatova str., 220045 Minsk, Belarus,
[2]Friedrich-Schiller-Universität, Max-Wien-Platz 1, D-07743 Jena, Germany
[3]Al-Farabi Kazakh National University, NNLOT, al-Farabi 71, 050040 Almaty
e-mail: komarov@bsu.by

Formation of ZnSe nanoclusters in the layers of silicon dioxide by high-fluence ion implantation and annealing

Abstract. In this work we used the method of "hot" implantation of zinc and selenium ions into SiO2 / Si structures in combination with subsequent heat treatment in order to form nanosized phases. Implantation modes for ionic synthesis chosen in such a way that the concentration of the embedded impurity is maximum approximately at the middle of the thickness of the dielectric layer. For the subsequent clustering of the impurity, it is necessary to create a high concentration of the implanted impurity at the maximum of the depth profile. The computer stimulation to select Implantation modes was carried out using the SRIM-2013 program. Also we calculated the thickness of the silicon dioxide layer sprayed during high-dose implantation of zinc ions was. In this way, we have studied the formation of ZnSe precipitates in silicon dioxide by means of Zn (150 keV, 4×1016 cm−2) and Se (170 keV, 4×1016 cm−2) implantation at 550 °C and subsequent annealing at 1000 °C for 3 min. From analysis of XTEM images it has been showen that the use of "hot" implantation leads to the formation of small nanoclusters with sizes from 2 to 15 nm. Subsequent annealing results in the redistribution of nanoclusters within the implanted layer and the formation of large crystallites (up to 80 nm). To analyze the distribution of the introduced impurity throughout the sample depth the Rutherford backscattering (RBS) method was used. The band at 251-256 cm-1 associated with LO phonons of crystal ZnSe was registered in Raman spectra.
Key words: Ion Implantation, nanoclusters, precipitates, silicon dioxide, zinc ions.

Introduction

Investigations aimed at the development of new light-emitting elements and devices based on silicon technology draw increasingly greater attention. Silicon is an indirect-gap semiconductor, and, as a result, has a low quantum efficiency of interband radiative recombination. Therefore, at the present time, various methods and approaches are used to create silicon-based light-emitting structures: creation of Si / SiO_2 superlattices [1], formation of silicon/germanium structures [2], silicon or germanium nanoprecipitates in SiO_2 [3,4], formation of nanocrystals of A^3B^5 compounds in silicon [5], and A^2B^6 compounds in SiO_2 [6]. In order to create new optoelectronic devices, A^2B^6 compounds based on chalcogenides, such as ZnS, CdSe, CdTe, and ZnSe, attracted great interest of scientific groups. This type of compounds has a direct-gap semiconductor structure and is now widely used for creation of lasers [7], solar cells [8], monochrome and white LEDs [9]. A perspective direction is combination of optical characteristics of these compounds with instrument silicon structures.

Zinc selenide (ZnSe) is of interest as a promising luminescent material for creation of various optoelectronic elements used in the visible and infrared spectral ranges, as well as in optical and laser CO_2 optics [10]. In works [11-12] it was reported about the creation of devices based on wide-gap semiconductors of ZnS and zinc selenide (ZnSe). Zinc selenide can be used for inorganic passivation [11] of various nanoclusters (quantum dots) to form a core-shell structure. Alloying of ZnS with various impurities gives electroluminophores with green, red and blue emission bands [12], the composition of which enables us to create an electroluminescent indicator with white light.

In this work ion-beam synthesis was used to form nanoscale inclusions of zinc selenide in silicon dioxide. It was assumed that the use of high-dose implantation of zinc and selenium ions in combination with subsequent heat treatment would enable us to synthesize extended layers of ZnSe nanoclusters in the SiO_2 matrix.

 Printed in Kazakhstan

Experimental conditions

In this work we used the method of "hot" implantation of zinc and selenium ions into SiO_2 / Si structures in combination with subsequent heat treatment in order to form nanosized phases.

The original 2 × 2 cm^{-2} samples were cut out from thermally oxidized SiO_2 (600 nm) / Si silicon wafers and implanted with ions under computer-simulated (SRIM-2013) modes in order to create a comparable concentration of zinc and selenium atoms at a given depth in the SiO_2 layer. Two groups of samples were made. For the first group, double implantation of ions in the SiO_2 (600 nm) / Si structure was made in the Zn ↓ (150 keV, 4 × 10^{16} cm^{-2}) + Se ↓ (170 keV, 4 × 10^{16} cm^{-2}) sequence. In the second part of the samples, the order of implantation was changed: Se ↓ + Zn ↓. For all samples, implantation was carried out at a temperature of 550 ° C - "hot" conditions. Post-implantation annealing was made in an argon atmosphere at 1000 ° C for 3 minutes.

To analyze the distribution of the introduced impurity throughout the sample depth the Rutherford backscattering (RBS) method was used.

The RBS spectra were recorded on the electrostatic accelerator complex AN-2500, created in the laboratory of elionics of the NIIPPP at A.N. Sevchenko Belarusian State University. From the experimentally obtained RBS spectra, profiles of impurity distribution in implanted SiO_2/Si structures were calculated. The profiles were calculated by modeling the RBS spectra using the HEAD software package until they completely coincided with the experimental spectra. When calculating the impurity profiles, the silicon oxide film was divided into several layers in order to more accurately determine the concentration of atoms over the thickness of the silicon dioxide layer.

Structural-phase transformations were studied by transmission electron microscopy (TEM) using a HitachiH-800 electron microscope with an accelerating voltage of 200 keV in the cross-section and Raman scattering geometry. The samples were prepared in two stages: mechanical polishing using the GATAN preparation system and subsequent thinning by ion etching.

Results of investigation

Implantation modes for ionic synthesis should be chosen in such a way that the concentration of the embedded impurity is maximum approximately at the middle of the thickness of the dielectric layer. For the subsequent clustering of the impurity, it is necessary to create a high concentration of the implanted impurity at the maximum of the depth profile.

Computer simulation of implantation of zinc ions into the SiO_2/Si structure in silicon dioxide was carried out using the SRIM-2013 program.

In the course of the work, it was planned to implant zinc and selenium ions into thin (less than 90 nm thick) and thick (300 - 900 nm) layers of silicon dioxide. Therefore, profiles were simulated for different energies of the implanted ions and doses in the range (5-10) × 10^{16} cm^{-2}.

The distribution of the implanted impurity in the SiO_2 and Si matrices was simulated for the energies of zinc ions from 80 to 200 keV. Figure 1 shows the calculated depth profiles of zinc impurity distribution in the SiO_2 matrix (SiO_2/Si structure with a 600 nm layer of silicon dioxide).

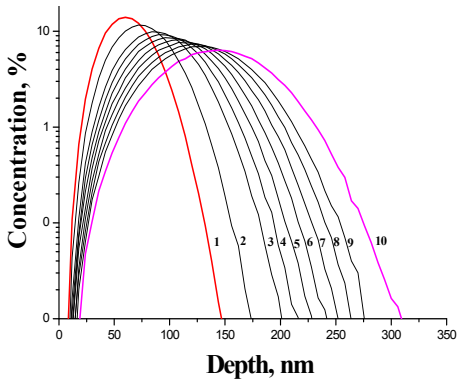

Figure 1 – Calculated (SRIM-2013) depth profiles of distribution of the impurity in silicon dioxide implanted with zinc ions with an energy of 80 (1), 100 (2), 120 (3), 130 (4), 140 (5), 150 (6), 160 (7), 170 (8), 180 (9), and 200 keV (10) at a dose of 4×10^{16} cm^{-2}

It can be seen from the figure that at the same dose of implantation, the zinc concentration at the maximum of the depth profile increases as the ion energy decreases. Thus, at an energy of 80 keV and a dose of 4 × 10^{16} cm^{-2} of zinc ions, respectively, the maximum concentration of zinc atoms in silicon dioxide at a depth of about 60 nm is about 15 at.%. For the same dose at an ion energy of 200 keV, the maximum concentration of zinc atoms in silicon dioxide at a depth of ~ 140 nm is about 7 at.%.

Thus, in accordance with the simulation data, the concentration of the implanted zinc impurity in silicon dioxide was changed from 7 to 30 at.% by changing the energy and ion doses in the ranges (80-200 keV) and (4-10) x 10^{16} cm^{-2}.

The thickness of the silicon dioxide layer sprayed during high-dose implantation of zinc ions was also

calculated. The calculation was carried out using the formula:

$$D_{distr} = \frac{Y}{N} \cdot D \quad (1)$$

where Y is the sputtering coefficient, N is the matrix density, and D is the implantation dose of the impurity ions.

The density of silicon dioxide was assumed to be 2.3 g / cm^3, which corresponds to 6.915 × 10 ^{23} at / cm^3.

Figure 2 shows the TEM micrograph (Figure 2A) of the cross section and the Raman spectrum (Figure 2B) of the SiO_2 layer immediately after implantation of the impurity in the sequence Zn ↓ + Se ↓. Under the near-surface layer of oxide free from precipitates (thickness 20-40 nm), there is an extended layer (40-190 nm from the surface) containing a large number of small clusters with sizes from 2 to 15 nm. At the center of this layer (region Rp ~ 100 nm) clusters are larger, their sizes are 8-15 nm. A similar picture was observed in our work [11], where larger clusters were formed in the region of a larger impurity concentration during implantation of zinc ions into the layers of silicon dioxide.

The Raman spectrum has two peaks. The intense narrow band at ~300 cm^{-1} corresponds to the well-known second-order Raman band (2TA) from the silicon substrate. The second peak with a maximum at 251-256 cm^{-1} corresponds to scattering by a longitudinal optical phonon (LO-mode) in crystalline ZnSe [12-14].

Thus, after implantation of zinc and selenium ions at a substrate temperature of 550 □, the ZnSe phase is formed, which in the matrix of silicon dioxide forms tiny nanoprecipitates recorded on TEM images.

A similar situation is observed in the samples with a different sequence (Se ↓ + Zn ↓) of implantation of an impurity in SiO_2 under the same "hot" implantation conditions (Figure 3). In this case, the thickness of the layer containing small (from 2 nm and larger) nanoclusters is noticeably smaller (the layer lies at a depth of about 20-140 nm from the surface), and the cluster sizes near R_p are larger (10-20 nm). It can be assumed that the selenium atoms implanted first prevent zinc diffusion into the depth of the sample during subsequent implantation due to formation of a ZnSe compound in which Zn atoms are less mobile. Localization of the impurity in a narrower layer also leads to an increase in the size of precipitates of the crystalline ZnSe phase, the presence of which is indicated by a peak near 251-256 cm^{-1} in the Raman spectrum (Figure 2B). It can be noted that in this case the intensity of this peak is lower than for the sequence (Zn ↓ + Se ↓) of implantations. The lower intensity of this peak can be explained both by the smaller fraction of formed ZnSe phase and by the greater number of structural defects in the precipitates (in comparison with the first sequence of introduction of impurities into the samples).

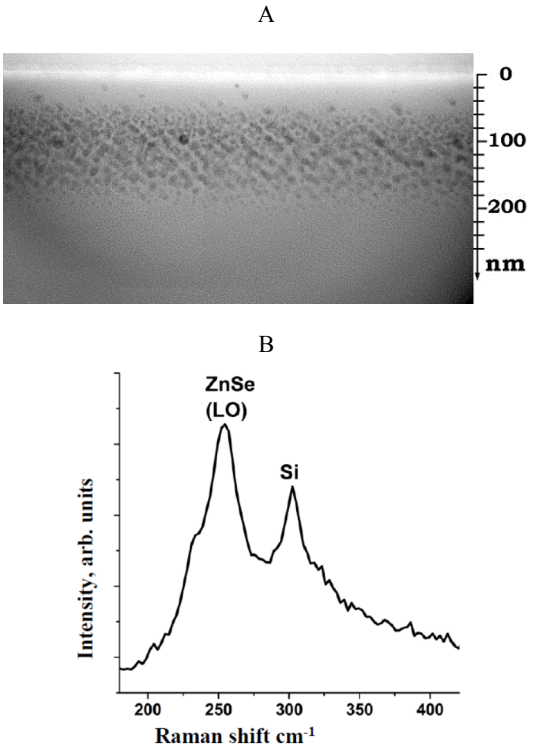

Figure 2 – TEM microphotograph of the cross section (A) and the Raman spectrum (B) after "hot" implantation of the impurity in the sequence Zn ↓ + Se ↓ into the SiO_2 layer

Figure 4 shows TEM-microphotographs of sample cross-sections after high-temperature annealing. It can be seen that there is a significant rearrangement of the structure of clusters for two samples with different sequences of impurity implantations.

The number (density) of clusters in the silicon dioxide layers sharply decreases, but their size substantially increases (up to 50-60 nm). Clusters are characterized by a regular faceted shape, and secondary structure defects (twin boundaries) are noticeable, which indicates their crystal structure. For the sample with the first type of implantation sequence (Zn ↓ + Se ↓), the depth shift of large clusters from the R_p region (~ 100 nm) to the surface (to a depth of ~ 60-70 nm) can be noted. Smaller (20-

40 nm) single clusters are recorded in other regions of the sample, which can be traced down to the SiO_2 (600 nm)/Si structure boundary. In the second sample (with the sequence of implants (Se ↓ + Zn ↓) large clusters near R_p were formed after heat treatment, in this case, single clusters with smaller dimensions in other places of the oxide layer were practically not registered, but in some spots on the surface of the sample release of impurities (Figure 2B - arrow), presumably, selenium was observed.

Raman spectra from samples after high-temperature annealing (Figure 5) are very similar to the spectra of samples immediately after implantation. Only 2 peaks are recorded: one is associated with the silicon substrate, the other – with the longitudinal mode of the optical phonon (LO-mode) in crystalline ZnSe.

The intensity of the band associated with the (LO)-mode of the optical phonon in ZnSe after heat treatment, like for samples immediately after implantation, is much lower for the sample with the second implantation sequence. This enables us to speak of a smaller amount of the ZnSe phase in this case.

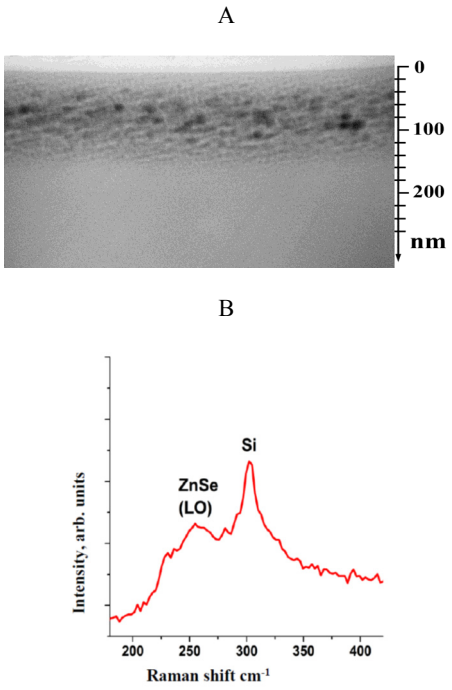

Figure 3 – TEM microphotograph of the cross section (A) and the Raman spectrum (B) after "hot" implantation of the impurity in the sequence Se ↓ + Zn ↓ into the SiO_2 layer

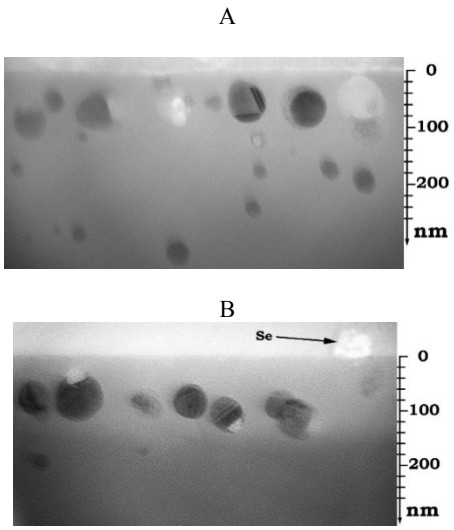

Figure 4 – TEM-microphotographs of the cross-section of SiO_2 layers after 550 ° C implantation: A - Zn + Se, B - Se + Zn; and after annealing in the BTT mode (1000 ° C, 3 min, Ar)

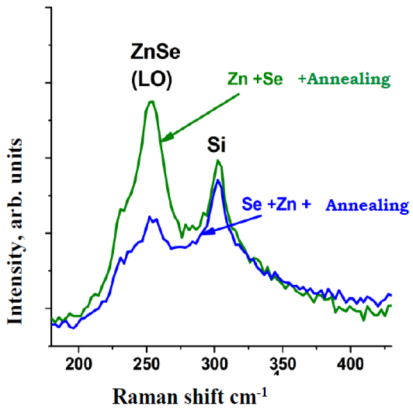

Figure 5 – Raman spectra from SiO_2 layers after 550 ° C implantation and annealing in BTT mode (1000 ° C, 3 min, Ar)

Conclusion

The structural and phase characteristics of silicon dioxide layers after high-dose implantation (at 550 ° C) of zinc and selenium ions with subsequent heat treatment have been studied. It was established that the use of "hot" implantation conditions leads to formation of small (2-15 nm) nanoclusters immediately after implantation of zinc and selenium ions. Subsequent high-temperature heat treatment leads to structural rearrangement and increase in cluster sizes (up to 80 nm).

In the Raman spectra of the samples, both immediately after implantation and after heat treatment, a band at 251-256 cm^{-1}, which corresponds to scattering by a longitudinal optical phonon (LO mode) of crystalline ZnSe, is registered.

This work was supported by the BRFFR grant for young scientists No. F17M-053.

References

1. X. Luo., S. B. Zhang., S. H. Wei. Chemical Design of Direct-Gap Light-Emitting Silicon // Phys. Rev. Lett. – 2002. – Vol. 89. – P. 076802.

2. L. Vescan., T. Stoica. Room-temperature SiGe light-emitting diodes // J. Luminescence. 1999. V. 80 P. 485-489.

3. F.L. Bregolin., M. Behar., U.S. Sias., E.C. Moreira. Photoluminescence induced from hot Ge implantation into SiO2 // Nucl. Instr. Meth. B. – 2009. – Vol. 267. – P. 1321-1323.

4. L. Rebohle. J. Von Borany. H. Fröb. W. Skorupa. Blue photo- and electroluminescence of silicon dioxide layers ion-implanted with group IV elements // J. Appl. Phys. B. 2000. V. 71. P. 131-151.

5. F.F. Komarov., L.A. Vlasukova., W. Wesch. et al. Influence of implantation and therapeutic modes for visible photoluminescency Zn (Se, S) nanoclusters in SiO2 // Nucl. Instr. Meth. B. – 2008. – Vol. 266. – P. 3557-3564.

6. I. D. Desnica-Frankovic., P. Dubcek. et. al. Influence of stoichiometry deviations on properties of ion-beam synthesized CdSe QDs // Nucl. Instr. Meth. B. 2005. V. 238. P. 302-305.

7. M.A. Haase., J. Qiu., J.M. Depuydt., H. Cheng Blue-green laser diodes // Appl. Phys. Lett. – 1991. – Vol. 59. – P. 1272.

8. H. Babucke., P. Thiele., T. Prasse., M. Rabe., F. Henneberger ZnSe-based electro-optic waveguide modulators for the blue-green spectral range // Semiconductor Science and Technology. – 1998. – Vol. 13. –P. 200-206.

9. I.K. Vereshchagin., B.A. Kovalev., L.A. Kosyachenko et. al. Elektrolyuminestsentnyye istochniki sveta // M.: Energoatomizdat. – 1990. – P. 168.

10. C.K.N. Patel. Continius-wave laser action on vibrational-rotational transitions onCO2 // Physical Review. – 1996. – Vol. 136. – P. A1187–A1193.

11. M. Makhavikou., F. F. Komarov., L. A. Vlasukova. et al. High Temperature Material Processes: An International Quarterly of High-Technology Plasma Processes. – 2014. – Vol. 18. – P. 255-261.

12. K. Shahad., D.J. Olego., C.G. Van De Walle., D.A. Cammack. Effects of strain on the optical and vibrational properties of ZnSe-ZnSxSe1-x strained-layer superlattices // J. Luminescence. 1990. V. 46. P. 109-136.

13. S. Itoh., K. Nakano. A. Ishibashi Current status and Future prospects of ZnSe-based light-emitting devices // Journal of Crystal Growth. – 2000. – Vol. 214. – P. 1029-1034.

14. K.T. Yong. Mn-doped near-infrared quantum dots as multimodal targeted probes for pancreatic cancer imaging // Nanotechnology. – 2009. – Vol. 20. – P. 1-10.